ISSN 1070-3284, Russian Journal of Coordination Chemistry, 2017, Vol. 43, No. 11, pp. 753–764. © Pleiades Publishing, Ltd., 2017.
Original Russian Text © A.S. Burlov, V.G. Vlasenko, S.I. Levchenkov, E.V. Korshunova, S.A. Mashchenko, Ya.V. Zubavichus, A.L. Trigub, T.V. Lifintseva, 2017, published in Koordinatsionnaya Khimiya, 2017, Vol. 43, No. 11, pp. 684–695.

Copper, Cobalt, and Nickel Complexes of Azomethine Compounds Containing Phenylazo Group in the Amine Fragment: Syntheses, Structures, and Magnetic Properties

A. S. Burlov[a], *, V. G. Vlasenko[b], S. I. Levchenkov[c], E. V. Korshunova[a], S. A. Mashchenko[a], Ya. V. Zubavichus[d], A. L. Trigub[d], and T. V. Lifintseva[e]

[a] *Research Institute of Physical and Organic Chemistry, Southern Federal University, Rostov-on-Don, Russia*
[b] *Research Institute of Physics, Southern Federal University, Rostov-on-Don, Russia*
[c] *Southern Scientific Center, Russian Academy of Sciences, Rostov-on-Don, Russia*
[d] *National Research Center "Kurchatov Institute", pl. Kurchatova 1, Moscow, 123182 Russia*
[e] *Southern Federal University, Rostov-on-Don, Russia*
**e-mail: anatoly.burlov@yandex.ru*

Received May 30, 2017

Abstract—The Cu, Ni, and Co complexes based on the following new azomethine compounds containing azobenzene groups in the *ortho*- or *para*-positions of the amine fragment are synthesized: 2-allyl-6-[(*E*)-[4-(*E*)-phenylazophenyl]iminomethyl]phenol (HL^1), 2-allyl-6-[(*E*)-[4-methyl-2-[(*E*)-phenylazo]-*p*-tolylazo]iminomethyl]phenol (HL^2), 5-methoxy-2-[(*E*)-[4-[(*E*)-phenylazo]phenyl]iminoethyl]phenol (HL^3), and 5-methoxy-2-[(*E*)-[4-methyl-2-[(*E*)-*p*-tolylazo]phenyl]iminomethyl]phenol (HL^4). The structures of the complexes are determined by the data of IR and ^{1}H NMR spectroscopy (for the azomethine compounds), X-ray absorption spectroscopy, and magnetochemistry. The coordination centers of all Cu complexes have a distorted square structure. A direct dependence of the geometry of the coordination polyhedron on the position of azobenzene groups in the amine fragments of the ligands is found for the Ni and Co complexes. The octahedral environment of the nickel and cobalt ions takes place in the case of the *ortho*-position of the amine fragment, whereas the square environment for the Ni complexes or the tetrahedral environment for the Co complexes is observed at the *para*-position. The molecular structures of two azomethines HL^1 and HL^4 are determined by X-ray diffraction analysis (CIF files CCDC nos. 1552836 (HL^1) and 1552837 (HL^4)).

Keywords: azomethines, metal complexes, X-ray absorption spectroscopy, X-ray diffraction analysis, magnetochemistry

DOI: 10.1134/S1070328417110021

INTRODUCTION

Azo compounds of the aromatic and heterocyclic series and their metal complexes attract attention of researchers due to both fundamental and practical significance [1–7]. For example, azylazobenzimidazoles and their complexes are photostable cationic dyes for polyacrylonitrile fiber [8, 9]. Azo compounds and their metal complexes are efficient additives to lubricating oils improving their load, antiwear, and antifriction characteristics [10]. On the one hand, the concepts about intrachelate isomerism, viz., a possibility of metallocycles with different unit contents to exist in one chelate molecule, were formulated and developed on the basis of the complexes with azo ligands [5–7, 11–13]. On the other hand, azomethine ligands are important objects of the modern chemistry of metal complexes, which is considered in a number of monographs and reviews [1, 3, 4, 13, 14]. The complexes of azomethine ligands with various functional properties, such as high catalytic activity in diverse reactions at high (>100°C) temperatures [15–17], are widely presented among biocoordination systems [18–21]. The presence of the azobenzene group, which is not involved in coordination with the metal, in the molecule of the complex with the azomethine ligand, is significant in studies of molecular magnetic materials and systems exhibiting an effect of thermo- and photoinduced crossover. The ability of the azobenzene fragment to undergo photoinduced *E*/*Z* isomerization is very important for the production of coordination compounds with the properties of molecular switches and photoactive materials [22–26].

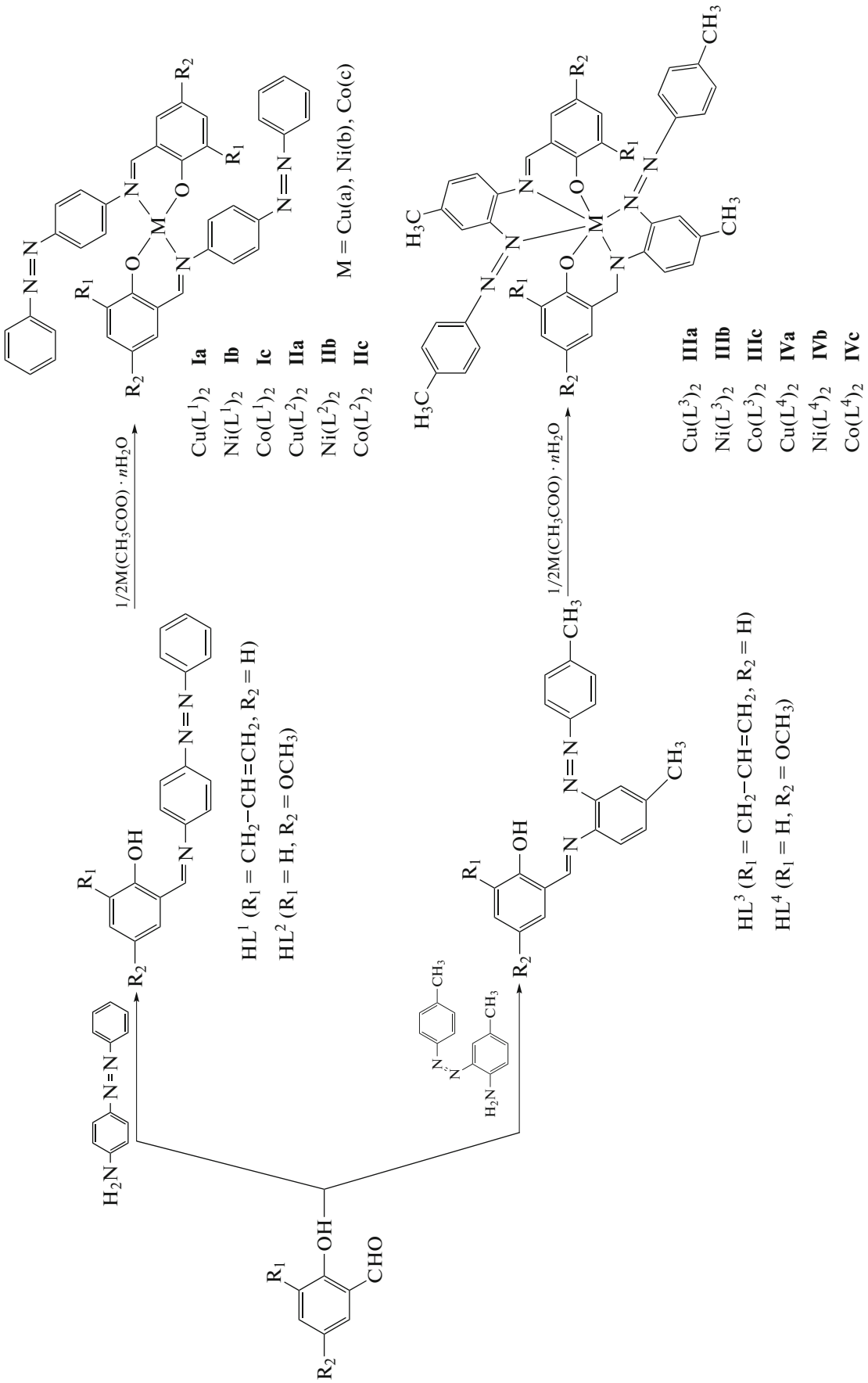
1/2M(CH3COO) · nH2O
Cu(L1)2 Ia
Ni(L1)2 Ib
Co(L1)2 Ic
Cu(L2)2 IIa
Ni(L2)2 IIb
Co(L2)2 IIc
M = Cu(a), Ni(b), Co(c)
HL1 (R1 = CH2–CH=CH2, R2 = H)
HL2 (R1 = H, R2 = OCH3)
1/2M(CH3COO) · nH2O
Cu(L3)2 IIIa
Ni(L3)2 IIIb
Co(L3)2 IIIc
Cu(L4)2 IVa
Ni(L4)2 IVb
Co(L4)2 IVc
HL3 (R1 = CH2–CH=CH2, R2 = H)
HL4 (R1 = H, R2 = OCH3)

Azomethine compounds and their metal complexes containing the azobenzene group in the aldehyde and amine fragments are of special interest. The azo group can participate in coordination to the metal in the complexes containing the phenylazo group in the *ortho*-position of the amine fragment, depending on the metal nature [27–31].

Continuing earlier works [24, 25, 27–29], we synthesized new compounds containing azobenzene groups in the *ortho*- or *para*-positions of the amine fragment, namely, 2-allyl-6-[(*E*)-[4-(*E*)-phenylazophenyl]iminomethyl]phenol (HL^1), 2-allyl-6-[(*E*)-[4-methyl-2-[(*E*)-phenylazo]-*p*-tolylazo]iminomethyl]phenol (HL^2), 5-methoxy-2-[(*E*)-[4-[(*E*)-phenylazo]phenyl]iminoethyl]phenol (HL^3), and 5-methoxy-2-[(*E*)-[4-methyl-2-[(*E*)-*p*-tolylazo]phenyl]iminomethyl]phenol (HL^4), and the related Cu (**Ia–IVa**), Ni (**Ib–IVb**), and Co (**Ic–IVc**) complexes. Their structures and magnetic properties were studied.

EXPERIMENTAL

Commercially available (AlfaAesar, Lancaster) 3-allylsalicylaldehyde, 5-methoxysalicylaldehyde, 4-aminoazobenzene, 6-amino-4,4-dimethylazobenzene, $Cu(CH_3COO)_2 \cdot H_2O$, $Ni(CH_3COO)_2 \cdot 4H_2O$, and $Co(CH_3COO)_2 \cdot 4H_2O$ were used.

Synthesis of HL^1–HL^4. 4-Aminoazobenzene (1.97 g, 0.01 mol) or 6-amino-4,4'-dimethylazobenzene (2.25 g, 0.01 mol) in ethanol (20 mL) was added to a solution of 3-allylsalicylaldehyde (1.62 g, 0.01 mol) or 5-methoxysalicylaldehyde (1.52 g, 0.01 mol), respectively, in ethanol (20 mL). The mixture was refluxed for 2 h. Precipitates formed on cooling were filtered off and recrystallized from a chloroform–methanol (1 : 2) system.

HL^1: yield 2.89 g (86%), orange crystals, mp = 101–102°C. IR (ν, cm^{-1}): 1610 (CH=N), 1282 (Ph–O). ^1H NMR ($CDCl_3$), δ, ppm: 3.51 (2H, d, J = 6.64 Hz, CH_2), 5.10–5.17 (2H, m, CH_2), 6.08 (1H, q, J = 9.0 Hz, CH), 6.93(1H, t, J = 7.5 Hz, C_{Ar}–H), 7.26–7.57 (7H, m, C_{Ar}–H), 7.92–8.03 (4H, m, C_{Ar}–H), 8.71 (1H, s, CH=N), 13.45 (1H, s, OH).

For $C_{22}H_{19}N_3O$

Anal. calcd., %:	C, 77.40;	H, 5.61;	N, 12.31.
Found, %:	C, 77.42;	H, 5.68;	N, 12.35.

HL^2: yield 2.48 g (75%), orange crystals, mp = 174–175°C. IR (ν, cm^{-1}): 1614 (CH=N), 1270 (Ph–O). ^1H NMR ($CDCl_3$), δ, ppm: 3.83 (3H, s, CH_3), 6.93–7.03 (3H, m, C_{Ar}–H), 7.26–7.56 (5H, m, C_{Ar}–H), 7.92–8.03 (4H, m, C_{Ar}–H), 8.67 (1H, s, CH=N), 12.65 (1H, s, OH).

For $C_{20}H_{17}N_3O_2$

Anal. calcd., %:	C, 72.49;	H, 5.17;	N, 12.68.
Found, %:	C, 72.52;	H, 5.28;	N, 12.71.

HL^3: yield 2.77 g (75%), red crystals, mp = 89–90°C. IR (ν, cm^{-1}): 1614 (CH=N), 1272 (Ph–O). ^1H NMR ($CDCl_3$), δ, ppm: 2.44 (6H, d, J = 3.6 Hz, CH_3), 3.53 (2H, d, J = 6.6 Hz, CH_2), 5.09–5.20 (2H, m, CH_2), 6.10 (1H, q, J = 9.0 Hz, CH), 6.88 (1H, t, J = 7.5 Hz, C_{Ar}–H), 7.26–7.34 (6H, m, C_{Ar}–H), 7.60 (1H, s, C_{Ar}–H), 7.88 (2H, d, J = 8.4 Hz, C_{Ar}–H), 8.62 (1H, s, CH=N), 14.15 (1H, s, OH).

For $C_{24}H_{23}N_3O$

Anal. calcd., %:	C, 78.02;	H, 6.27;	N, 11.37.
Found, %:	C, 78.15;	H, 6.12;	N, 11.42.

HL^4: yield 3.1 g (75%), red crystals, mp = 152–153°C. IR (ν, cm^{-1}): 1619 (CH=N), 1270 (Ph–O). ^1H NMR ($CDCl_3$), δ, ppm: 2.44 (6H, d, J = 5.1 Hz, CH_3), 3.80 (3H, s, CH_3), 6.83–7.33 (7H, m, C_{Ar}–H), 7.58 (1H, s, C_{Ar}–H), 7.86 (2H, d, J = 8.4 Hz, C_{Ar}–H), 8.59 (1H, s, CH=N), 13.29 (1H, s, OH).

For $C_{22}H_{21}N_3O_2$

Anal. calcd., %:	C, 71.52;	H, 5.89;	N, 11.64.
Found, %:	C, 73.48;	H, 5.92;	N, 11.59.

Synthesis of metal complexes. Copper acetate monohydrate (0.10 g, 0.5 mmol), or nickel acetate tetrahydrate (0.124 g), or cobalt acetate tetrahydrate (0.125 g) in ethanol (20 mL) was added to a solution of HL^1 (0.34 g, 1 mmol), or HL^2 (0.33 g), or HL^3 (0.37 g), or HL^4 (0.36 g), respectively, in ethanol (30 mL). The mixture was refluxed for 3 h. Precipitates of the complexes formed on cooling were filtered off, washed two times with boiling ethanol (5 mL), and recrystallized from a dichloromethane–ethanol (2 : 1) system.

Bis{2-allyl-6-[(*E*)-[4-(*E*)-phenylazophenyl]iminomethyl]phenolato}copper(II) (Ia): yield 0.6 g (80%), brown crystals, mp = 207–208°C, μ_{eff} = 1.92 μ_B (293 K). IR (ν, cm^{-1}): 1600 (CH=N), 1327 (Ph–O).

For $C_{44}H_{36}CuN_6O_2$

Anal. calcd., %:	C, 71.00;	H, 4.87;	N, 11.29;	Cu, 8.53.
Found, %:	C, 71.01;	H, 4.90;	N, 11.32;	Cu, 8.60.

Bis{2-allyl-6-[(*E*)-[4-(*E*)-phenylazophenyl]iminomethyl]phenolato}nickel(II) (Ib): yield 0.52 g (70%), brown powder, mp = 202–203°C, diamagnetic (293 K). IR (ν, cm^{-1}): 1603 (CH=N), 1328 (Ph–O).

For $C_{44}H_{36}NiN_6O_2$

Anal. calcd., %: C, 71.46; H, 4.91; N, 11.36; Ni, 8.01.
Found, %: C, 71.52; H, 4.98; N, 11.45; Ni, 8.01.

Bis{2-allyl-6-[(*E*)-[4-(*E*)-phenylazophenyl]iminomethyl]phenolato}cobalt(II) (Ic): yield 0.61 g (83%), red-brown powder, mp = 196–197°C, μ_{eff} = 4.59 μ_B (293 K). IR (ν, cm^{-1}): 1600 (CH=N), 1292 (Ph–O).

For $C_{44}H_{36}CoN_6O_2$

Anal. calcd., %: C, 71.44; H, 4.90; N, 11.36, Ni, 7.97.
Found, %: C, 71.52; H, 4.99; N, 11.28, Ni, 7.89.

Bis{5-methoxy-2-[(*E*)-[4-[(*E*)-phenylazophenyl]iminoethyl]phenolato}copper(II) (IIa): yield 0.56 g (85%), brown powder, mp > 250°C, μ_{eff} = 1.92 μ_B (293 K). IR (ν, cm^{-1}): 1584 (CH=N), 1318 (Ph–O).

For $C_{40}H_{32}CuN_6O_4$

Anal. calcd., %: C, 66.33; H, 4.45; N, 11.60; Cu, 8.77.
Found, %: C, 66.45; H, 4.52; N, 11.71; Cu, 8.81.

Bis{5-methoxy-2-[(*E*)-[4-[(*E*)-phenylazophenyl]iminoethyl]phenolato}nickel(II) (IIb): yield 0.58 g (81%), red-brown powder, mp > 260°C, diamagnetic (293 K). IR (ν, cm^{-1}): 1589 (CH=N), 1311 (Ph–O).

For $C_{40}H_{32}NiN_6O_4$

Anal. calcd., %: C, 66.78; H, 4.48; N, 11.68; Ni, 8.16.
Found, %: C, 66.82; H, 4.51; N, 11.75; Ni, 8.26.

Bis{5-methoxy-2-[(*E*)-[4-[(*E*)-phenylazo]phenyl]iminoethyl]phenolato}cobalt(II) (IIc): yield 0.58 g (80%), red-brown powder, mp = 230–231°C, μ_{eff} = 4.36 μ_B (273 K). IR (ν, cm^{-1}): 1572 (CH=N), 1311 (Ph–O).

For $C_{40}H_{32}CoN_6O_4$

Anal. calcd., %: C, 66.76; H, 4.48; N, 11.68; Co, 8.19.
Found, %: C, 66.86; H, 4.41; N, 11.72; Co, 8.32.

Bis{2-allyl-6-[(*E*)-[4-methyl-2-[(*E*)-phenylazo]-*p*-tolylazo]iminomethyl]phenolato}copper(II) (IIIa): yield 0.74 g (88%), brown powder, mp > 250°C, μ_{eff} = 1.97 μ_B (293 K). IR (ν, cm^{-1}): 1600 (CH=N), 1292 (Ph–O).

For $C_{48}H_{44}CuN_6O_2$

Anal. calcd., %: C, 72.3; H, 5.54; N, 10.50; Cu, 7.94.
Found, %: C, 72.15; H, 5.35; N, 10.49; Cu, 8.05.

Bis{2-allyl-6-[(*E*)-[4-methyl-2-[(*E*)-phenylazo]-*p*-tolylazo]iminomethyl]phenolato}nickel(II) (IIIb): yield 0.7 g (88%), dark brown powder, mp > 250°C, μ_{eff} = 2.93 μ_B (293 K). IR (ν, cm^{-1}): 1612 (CH=N), 1336 (Ph–O).

For $C_{48}H_{44}NiN_6O_2$

Anal. calcd., %: C, 72.46; H, 5.57; N, 10.56; Ni, 7.38.
Found, %: C, 72.32; H, 5.61; N, 10.49; Ni, 7.42.

Bis{2-allyl-6-[(*E*)-[4-methyl-2-[(*E*)-phenylazo]-*p*-tolylazo]iminomethyl]phenolato}cobalt(II) (IIIc): yield 0.69 g (87%), dark brown powder, mp = 246–247°C, μ_{eff} = 4.36 μ_B (293 K). IR (ν, cm^{-1}): 1610 (CH=N), 1332 (Ph–O).

For $C_{48}H_{44}CoN_6O_2$

Anal. calcd., %: C, 72.44; H, 5.57; N, 10.56; Co, 7.41.
Found, %: C, 72.32; H, 5.68; N, 10.61; Co, 7.52.

Bis{5-methoxy-2-[(*E*)-[4-methyl-2-[(*E*)-*p*-tolylazo]phenyl]iminomethyl]phenolato}copper(II) (IVa): yield 0.58 g (74%), brown powder, mp > 250°C, μ_{eff} = 1.97 μ_B (293 K). IR (ν, cm^{-1}): 1602 (CH=N), 1317 (Ph–O).

For $C_{44}H_{40}CuN_6O_4$

Anal. calcd., %: C, 67.72; H, 5.17; N, 10.77; Cu, 8.14.
Found, %: C, 67.81; H, 5.20; N, 10.88; Cu, 8.34.

Bis{5-methoxy-2-[(*E*)-[4-methyl-2-[(*E*)-*p*-tolylazo]phenyl]iminomethyl]phenolato}nickel(II) (IVb): yield 0.69 g (89%), dark brown powder, mp > 250°C, μ_{eff} = 2.95 μ_B (293 K). IR (ν, cm^{-1}): 1606 (CH=N), 1303 (Ph–O).

For $C_{44}H_{40}NiN_6O_4$

Anal. calcd., %: C, 68.14; H, 5.20; N, 10.84; Ni, 7.57.
Found, %: C, 68.30; H, 5.28; N, 10.72; Ni, 7.38.

Bis{5-methoxy-2-[(*E*)-[4-methyl-2-[(*E*)-*p*-tolylazo]phenyl]iminomethyl]phenolato}cobalt(II) (IVc): yield 0.61 g (78%), dark brown powder, mp > 250°C, μ_{eff} = 4.47 μ_B (293 K). IR (ν, cm^{-1}): 1611 (CH=N), 1300 (Ph–O).

For $C_{44}H_{40}CoN_6O_4$

Anal. calcd., %: C, 68.12; H, 5.20; N, 10.83; Co, 7.60.
Found, %: C, 68.28; H, 5.31; N, 10.71; Co, 7.72.

Elemental analysis (C, H, N) was carried out on a Carlo Erba Instruments TCM 480 instrument. The IR spectra of samples in KBr pellets were recorded on a

Nicolet Impact-400 instrument in a range of 4000–400 cm^{-1}. Melting points were measured on a Kofler heating stage. ^1H NMR spectra were recorded on a Varian Unity 300 spectrometer with a working frequency of 300 MHz in the internal stabilization mode of the 2H polar-resonance line in $CDCl_3$ at 20°C. The specific magnetic susceptibility was determined by relative Faraday's method at room temperature using $Hg[Co(CNS)_4]$ as a standard for calibration.

The X-ray absorption Cu, Co, and Ni *K*-edges of compounds **I–IV** (a, b, c) were obtained at the Strukturnoe Materialovedenie station of the Kurchatov Synchrotron Radiation Source (Moscow) [32]. The X-ray absorption spectra were processed by standard procedures of background subtraction, normalization to the value of *K*-edge jump, and isolation of atomic absorption μ_0, after which the Fourier transform of the obtained extended X-ray absorption fine structure (EXAFS) χ spectrum was performed in the range of photoelectron wave vectors *k* from 2.5 to 12–13 $Å^{-1}$ with the weight function k^3. The obtained module Fourier transformant (MFT) of the EXAFS corresponded to the radial distribution function of the atoms around the absorbing metal ion with phase shift accuracy. The exact values of parameters of the nearest environment of the metal ion in the studied compounds were determined by nonlinear fitting of parameters of the corresponding coordination spheres when comparing the calculated EXAFS and that subtracted from the overall absorption spectrum by the Fourier filtration method. The nonlinear fitting was performed using the IFFEFIT program package [33]. The phases and amplitudes of photoelectron wave scattering necessary for the construction of the model spectrum were calculated using the FEFF7 program [34]. The X-ray data for single crystals of the complexes with the similar atomic environments of metal ions were used as the initial atomic coordinates necessary for the calculation of the scattering phases and amplitudes and further fitting. The search for these structures was performed in the Cambridge Structural Database.

X-ray diffraction analyses of HL^1 and HL^4 were carried out on a Bruker APEX-II diffractometer equipped with a CCD detector and a monochromatic radiation source (MoK_α, $\lambda = 0.71073$ Å, graphite monochromator) using the standard CrysAlisPro procedure [35]. The structures were solved by a direct method and refined in the full-matrix anisotropic approximation for all non-hydrogen atoms. Hydrogen atoms were localized from difference electron density syntheses and refined in the isotropic approximation. The main crystallographic data and refinement parameters are presented in Table 1. All calculations were performed using the SHELXS-97 program package [36]. The full array of X-ray diffraction data was deposited with the Cambridge Crystallographic Data Centre (CIF files CCDC no. 1552836 (HL^1) and 1552837 (HL^4); deposit@ccdc.cam.ac.uk or http://www.ccdc.cam.ac.uk/data_request/cif).

RESULTS AND DISCUSSION

Azomethine compounds HL^1–HL^4 were synthesized by the condensation in ethanol of 3-allylsalicylic or 5-methoxysalicylic aldehyde with 4-aminobenzene and 6-amino-4,4'-dimethylazobenzene at a molar ratio of 1 : 1 and recrystallized from a chloroform–ethanol (1 : 2) system.

Compounds HL^1–HL^4 are highly soluble in chloroform, dichloromethane, dimethyl sulfoxide, and dimethylformamide and are poorly soluble in ethanol and methanol.

The structures of compounds HL^1–HL^4 were established by elemental analyses and IR and ^1H NMR spectroscopy. The IR spectra of HL^1–HL^4 contain absorption bands at 1610–1619 cm^{-1} ν(CH=N) and 1270–1282 cm^{-1} ν(Ph–O). The signals of all protons according to the empirical formula were found in the ^1H NMR spectra. The signals of the CH=N protons at 8.71 (HL^1), 8.62 (HL^2), 8.67 (HL^3), and 8.59 (HL^4) ppm and the signals of the protons of the OH groups at 13.45 (HL^1), 14.15 (HL^2), 12.65 (HL^3), and 13.29 (HL^4) ppm, respectively, were detected.

The molecular structures of compounds HL^1 and HL^4 were determined by X-ray diffraction analysis (Fig. 1). Selected bond lengths and bond angles are given in Table 2. The lengths of the C–C bonds in the aromatic cycles and N(1)–N(2), N(3)–C(10), and C(21)–C(22) double bonds in a molecule of HL^1 are close to standard values [37].

On the whole, a molecule of HL^1 is nearly planar. The cycles bound by the azo group are almost coplanar (the dihedral angle between the mean planes is 1.83°). The phenol ring C(14)C(15)C(16)C(17)-C(18)C(19) is insignificantly turned relative to the C(7)C(8)C(9)C(10)C(11)C(12) cycle, so that the dihedral angle between the mean planes is 5.87°.

The very strong intramolecular hydrogen bond O(1)–H(1)···N(3) with the following parameters is observed in a molecule of compound HL^1: O(1)–H(1) 0.84, H(1)···N(3) 1.85, O(1)···N(3) 2.596(2) Å, and angle O(1)H(1)N(3) 147°.

Centrosymmetric pairs bound by the shifted stacking interaction are formed by molecules of compound HL^1 in single crystal. The dihedral angle between the

mean planes of the C(14)C(15)C(16)-=C(17)C(18)-C(19) and $C(1)^iC(2)^iC(3)^iC(4)^iC(5)^iC(6)^i$ cycles (symmetry procedure: $3/2 - x$, $1/2 - y$, $-z$) is 7.68°, and the intercentroid distance is 4.468 Å. The distance between the centroids of the C(7)C(8)C(9)C(10)-C(11)C(12) and $C(7)^iC(8)^iC(9)^i$-$C(10)^iC(11)^iC(12)^i$ cycles is 4.389 Å.

The bond lengths in a molecule of compound HL^4 are close to standard values (Table 2). As a whole, a molecule of HL^4 is not planar. The cycles bound by the azo group are not coplanar because of the turn relative to the N(2)–C(13) bond, and the dihedral angle between their mean planes is 23.29°. The phenol cycle C(1)C(2)C(3)C(4)C(5)C(6) and C(7)C(8)C(9)-C(10)C(11)C(12) cycle, in turn, are turned relative to the N(1)–C(8) bond, and the dihedral angle between the mean planes is 10.13°.

The strong intramolecular bond O(1)–H(1)···N(1) is also observed in a molecule of compound HL^4 (O(1)–H(1) 0.89, H(1)···N(1) 1.77, O(1)···N(1) 2.593(2) Å, angle O(1)H(1)N(1) 152°).

According to the elemental analysis data, metal complexes **I–IV** based on HL^1–HL^4 (a, b, c) have the composition ML_2. The changes characteristic of chelate structures are observed in the IR spectra of all complexes [38–40]. The ν(CH=N) stretching vibration bands of the ligands in a range of 1610–1619 cm^{-1} decrease by 2–10 cm^{-1} upon complex formation, whereas the ν(Ph–O) stretching vibration bands at 1272–1282 cm^{-1} increase by 30–60 cm^{-1} depending on the type of ligand.

Complexes **I** (a, c), **II** (a, c), **III** (a, b, c), and **IV** (a, b, c) are paramagnetic. The values of μ_{eff} at 293 K of the copper complexes are 1.92 (**Ia**), 1.92 (**IIa**), 1.97 (**IIIa**), and 1.97 (**IVa**) μ_B; those of the cobalt complexes are 4.59 (**Ic**), 4.36 (**IIc**), 4.36 (**IIIc**), and 4.47 (**IVc**) μ_B; and μ_{eff} of the nickel complexes are 2.93 (**IIIb**) and 2.95 (**IVb**) μ_B, which corresponds to the purely spin values of the magnetic moment taking into account the contribution of the orbital component. The values of μ_{eff} do not change with a decrease in temperature, indicating the mononuclear structure of these complexes. Nickel complexes **Ib** and **IIb** containing the azo group in the *para* position of the amine fragment of the ligand are diamagnetic at room temperature, which indicates their square structure.

As has previously been shown for the nickel complexes with similar ligands containing azo groups in the *ortho* position of the amine fragment, cyclometallated square structures of the coordination mode of type **V** take place [41].

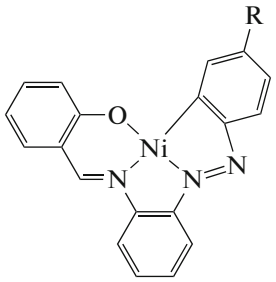

V R = H, CH_3

However, according to the elemental analysis data, nickel complexes **IIIb** and **IVb** have the composition NiL_2, and their magnetic moments are 2.93–2.95 μ_B, which are characteristic of the octahedral structure of the coordination mode.

The structure of the nearest atomic environment of metal ions in the coordination sites of complexes **I–IV** (a, b, c) was determined by the data of X-ray absorption spectroscopy from analysis of the X-ray absorption near edge structure (XANES) and EXAFS *K*-edges of these compounds. The normalized XANES Cu, Ni, and Co *K*-edges and the corresponding MFT EXAFS for complexes **I–IV** (a, b, c) are presented in Fig. 2. The pre-edge XANES structure and the first derivatives $d\mu/dE$, where μ is the mass absorption coefficient of X-ray radiation, are also shown in Fig. 2 (insets).

A comparison of the *K*-edge XANES for the studied samples shows that for the Ni and Co complexes they differ substantially in fine structure depending on the *ortho*- or *para*-position of the azobenzene group of the amine fragment in the ligand, whereas the Cu *K*-edge XANES are close in structure for all copper complexes. The XANES of the Ni complexes in which the azobenzene group is localized in the *para* position (**Ib**, **IIb**) are characterized by a low-intensity pre-edge peak *A* caused by the manifestation of the *p–d* mixing of the AO of the metal in the complex. The intensity of the pre-edge peak *A* in the XANES of the Ni complexes in which the azobenzene group is localized in the *ortho* position (**IIIb**, **IVb**) is also low. Such a low intensity of peak *A* is usually characteristic of the octahedral or square environment of the absorbing atom when its intensity is caused by very weak forbidden quadrupole electron transitions $3d \rightarrow 1s$. The determining distinction in the XANES of these two pairs of complexes is the presence of the intense peak *B* directly at the Ni *K*-edge of complexes **Ib** and **IIb** and its absence in the XANES of complexes **IIIb** and **IVb**. The presence of the intense well resolved peak *B* in the XANES is characteristic of the square coordination site in the complexes and is due to the manifestation of the vacant p_z-AO of the metal (axis $z \perp$ plane N_2O_2). The manifestation of this component *B*, along with a very

Table 1. Crystallographic data and experimental and refinement characteristics for compounds HL^1 and HL^4

Parameter	Value	
	HL^1	HL^4
FW	341.40	359.42
Crystal size, mm	0.33 × 0.22 × 0.09	0.43 × 0.23 × 0.11
Temperature, K	173(2)	150(2)
Crystal system	Monoclinic	Monoclinic
Space group	$C2/c$	$P2_1/n$
a, Å	43.1032(18)	12.5558(14)
b, Å	7.2874(3)	11.9430(13)
c, Å	11.5190(4)	13.3440(15)
β, deg	102.054(7)	113.114(2)
V, Å^3	3538.46	1840.4(4)
Z	8	4
ρ_{calcd}, g/cm^3	1.282	1.297
μ, mm^{-1}	0.081	0.085
F(000)	1440	760
Scan range over θ, deg	1.94–55.12	4.76–55.7
Number of measured reflections	7677	10316
Number of independent reflections	3998	4422
Number of reflections with $I > 2\sigma(I)$	2792	2957
Ranges of reflection indices	$-56 \le h \le 56$, $-6 \le k \le 9$, $-14 \le l \le 14$	$-14 \le h \le 16$, $-12 \le k \le 15$, $-17 \le l \le 17$
Number of refined parameters	235	251
R_1 ($I > 2\sigma(I)$)	0.0436	0.0483
wR_2 (all reflections)	0.1542	0.1346
GOOF (all reflections)	1.000	0.999
$\Delta\rho_{max}/\Delta\rho_{min}$, e Å^{-3}	0.355/–0.246	0.361/–0.202

low intensity of the pre-edge peaks *A*, suggests that the metal ion has a square atomic environment in nickel complexes **Ib** and **IIb**. The main absorption maximum *C* also demonstrates substantial differences in the XANES of complexes **Ib** and **IIb** compared to the XANES of complexes **IIIb** and **IVb**.

The changes in the shape of the XANES are especially pronounced for the Ni complexes when considering their first derivatives dμ/dE of the absorption Ni *K*-edges. For the XANES of complexes **Ib** and **IIb**, dμ/dE has several strongly split maxima, whereas dμ/dE of the absorption Ni *K*-edges of complexes **IIIb** and **IVb** have one broad maximum. These specific features of the first derivatives are also characteristic of the square or distorted octahedral environment of nickel ions.

Similar changes are observed for the XANES of Co complexes **I–IV** on changing the position of the azobenzene group of the amine fragment in the ligand. However, unlike the XANES of Ni complexes **Ib** and **IIb**, in the XANES of cobalt complexes **Ic** and **IIc** the intensity of the pre-edge peaks *A* is high and shoul-

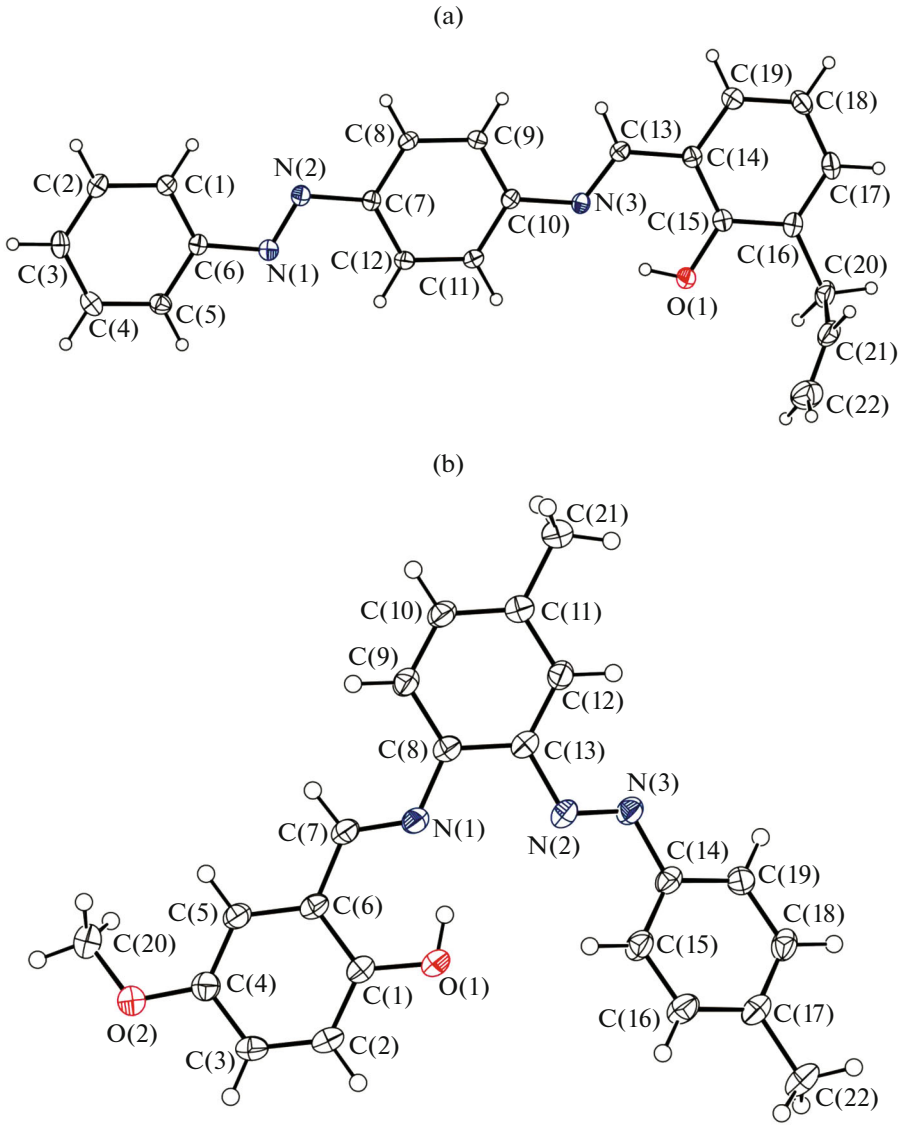

Fig. 1. Molecular structures of compounds (a) HL^1 and (b) HL^4 in the representation of atoms by thermal shift ellipsoids with 30% probability.

der *B* is nearly absent, being characteristic of the complexes in which metal ions have a tetrahedral distorted environment. All arguments for the XANES and their first derivatives dμ/dE of nickel complexes **IIIb** and **IVb** can be assigned to the interpretation of the XANES for complexes **IIIc** and **IVc**. The latter allows one to suggest that the octahedral environment of the cobalt ion takes place in these compounds.

The XANES shape and intensities of pre-edge peaks *A* for Cu complexes **I–IVa** remain almost unchanged depending on the *ortho*- or *para*-position of the azobenzene group of the amine fragment in the ligand, which is especially well seen from similar dμ/dE of the Cu *K*-edges of these complexes. These XANES characteristics of **I–IVa** are typical of a distorted square environment of the copper ions in the complexes.

This qualitative description of the local structure in complexes **I–IV** (a, b, c) on the basis of the consideration of the XANES was confirmed by an analysis of the EXAFS absorption *K*-edges of these compounds, which gave the quantitative characteristics of the structure of the nearest atomic environment of the absorbing metal ions. The MFT of the *K*-edge EXAFS are shown in Figs. 2d–2f, and the quantitative data on the parameters of the nearest coordination spheres in complexes **I–IV** (a, b, c) are presented in Table 3. All MFT have the main peak at $r = 1.46–1.54$ Å caused by

Table 2. Selected interatomic distances and bond angles in molecules based on HL^1 and HL^4

Bond	*d*, Å	Bond	*d*, Å
		HL^1	
O(1)–C(15)	1.3470(17)	N(2)–C(7)	1.4246(18)
N(1)–N(2)	1.2536(17)	N(3)–C(13)	1.2832(19)
N(1)–C(6)	1.4281(18)	N(3)–C(10)	1.4166(18)
		HL^4	
O(1)–C(1)	1.3544(19)	N(1)–C(8)	1.4120(19)
O(2)–C(4)	1.3690(19)	N(2)–N(3)	1.2505(18)
O(2)–C(20)	1.419(2)	N(2)–C(13)	1.4309(17)
N(1)–C(7)	1.278(2)	N(3)–C(14)	1.4346(17)
Angle	ω, deg	Angle	ω, deg
		HL^1	
C(15)O(1)H(1)	109.5	N(1)N(2)C(7)	114.56(12)
N(2)N(1)C(6)	113.91(12)	C(13)N(3)C(10)	122.40(13)
		HL^4	
C(1)O(1)H(1)	104.9(15)	N(2)N(3)C(14)	113.63(12)
C(4)O(2)C(20)	116.43(12)	N(1)C(7)C(6)	121.28(13)
C(7)N(1)C(8)	122.65(12)	O(1)C(1)C(2)	119.50(13)
N(3)N(2)C(13)	114.77(12)	O(1)C(1)C(6)	121.78(13)

photoelectron wave scattering on the nearest coordination sphere of the nitrogen and oxygen atoms of the ligands. The next peaks in the MFT at high *r* are related to the coordination spheres containing different atoms (mainly carbon atoms) of the ligands. The calculations of the model EXAFS showed that the nearest environment of the metal ions in complexes **I–IV** (a) and **I**, **II** (b, c) consisted of two nitrogen atoms and two oxygen atoms, the average distance to which are presented in Table 3. For Ni complexes **III**, **IV** (b) and Co complexes **III**, **IV** (c), the best model of the nearest atomic environment corresponded to the first coordination sphere of six oxygen and nitrogen atoms, indicating an additional coordination of two nitrogen atoms in the compounds in which the azobenzene group of the amine fragment in the ligand is localized in the *ortho* position. The average distances from the complexing metal to these nitrogen atoms are longer by 0.1–0.2 Å. The obtained values of Debye–Waller factors are typical of coordination spheres of these radii and compositions. The results are well consistent with the magnetochemical data for these complexes.

To conclude, the following new azomethine compounds containing azobenzene groups in the *ortho*- or *para*-position of the amine fragment were synthesized: 2-allyl-6-[(*E*)-[4-(*E*)-phenylazophenyliminomethyl]phenol, 2-allyl-6-[(*E*)-[4-(*E*)-phenylazo]-*p*-tolylazo]iminomethyl]phenol, 5-methoxy-2-[(*E*)-[4-[(*E*)-phenylazo]phenyl]iminoethyl]phenol, and 5-methoxy-2-[(*E*)-[4-methyl-2-[(*E*)-*p*-tolylazo]phenyl]iminomethyl]phenol. Their structures were determined by the data of IR spectroscopy, ^{1}H NMR spectroscopy, and X-ray diffraction analysis. The Cu, Ni, and Co complexes were synthesized on the basis of the above compounds. The structures of the complexes were established by X-ray absorption spectroscopy, and their magnetic properties were studied. The coordination sites of all Cu complexes were found to have a distorted square structure. A direct dependence of the coordination

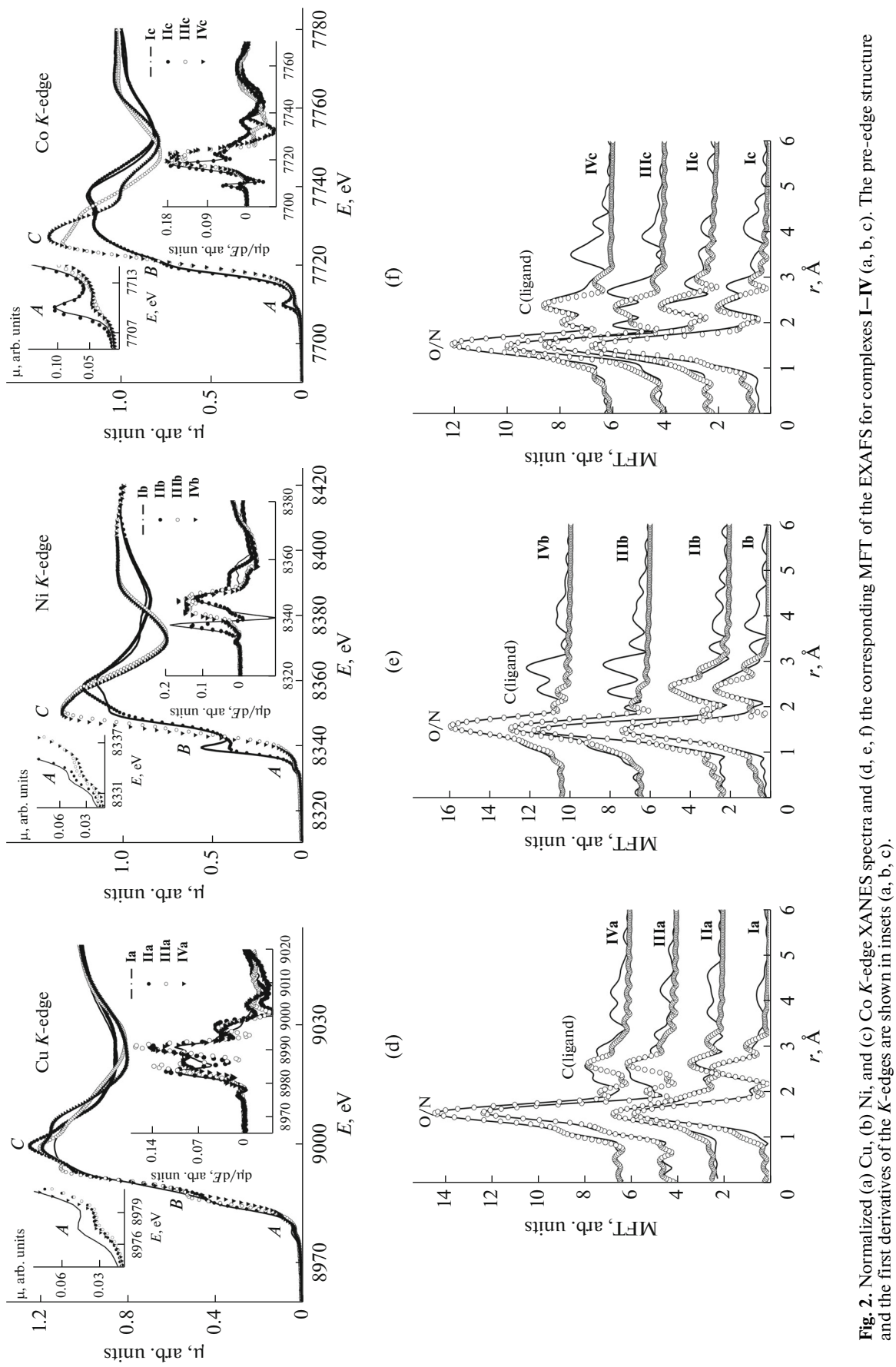

Fig. 2. Normalized (a) Cu, (b) Ni, and (c) Co *K*-edge XANES spectra and (d, e, f) the corresponding MFT of the EXAFS for complexes **I–IV** (a, b, c). The pre-edge structure and the first derivatives of the *K*-edges are shown in insets (a, b, c).

Table 3. Parameters of the local atomic environment of metal ions in **I–IV** (a, b, c) complexes obtained by the multisphere fitting of the EXAFS *K*-edges (*R* is interatomic distance, σ^2 is the Debye–Waller factor, and $\Re$ is the fitting goodness-of-fit)

Compound	*N*	*R*, Å	σ^2, Å^2	Coordination sphere	$\Re$, %
Ia	2	1.89	0.0044	O/N	3.2
	2	2.01	0.0044	O/N	
	6	2.90–2.97	0.0044	C	
IIa	2	1.85	0.0044	O/N	2.2
	2	2.01	0.0044	O/N	
	6	2.86–3.01	0.0044	C	
IIIa	2	1.89	0.0035	O/N	1.7
	2	1.99	0.0035	O/N	
	6	2.91–3.02	0.0035	C	
IVa	2	1.89	0.0037	O/N	1.3
	2	1.95	0.0037	O/N	
	6	2.90–3.05	0.0037	C	
Ib	2	1.84	0.0042	O/N	9.9
	2	1.96	0.0042	O/N	
	6	2.82–2.91	0.0042	C	
IIb	2	1.84	0.0038	O/N	4.3
	2	1.91	0.0038	O/N	
	6	2.81–2.90	0.0038	C	
IIIb	2	1.97	0.0050	O/N	2.3
	2	2.03	0.0050	O/N	
	2	2.05	0.0050	O/N	
IVb	2	2.00	0.0044	O/N	1.6
	2	2.06	0.0044	O/N	
	2	2.19	0.0044	O/N	
Ic	2	1.91	0.0044	O/N	7.1
	2	1.95	0.0044	O/N	
	6	2.83–2.96	0.0044	C	
IIc	2	1.92	0.0046	O/N	3.1
	2	1.97	0.0046	O/N	
	6	2.84–2.97	0.0046	C	
IIIc	4	2.00	0.0050	O/N	4.4
	2	2.12	0.0050	O/N	
	6	2.91–3.04	0.0050	C	
IVc	4	2.01	0.0050	O/N	6.6
	2	2.12	0.0050	O/N	
	6	2.92–3.05	0.0050	C	

polyhedron geometry on the position of the azobenzene groups in the amine fragment of the ligands was observed for the Ni and Co complexes. The octahedral environment of the nickel and cobalt ions is observed in the case of the *ortho*-position of the amine fragment, whereas the square environment for the Ni complexes or tetrahedral one for the Co complexes takes place in the case of the *para*-position.

ACKNOWLEDGMENTS

This work was supported financially by the Ministry of Education and Science of the Russian Federation (Project no. 3.6105.2017/8.9).

REFERENCES

1. Nejati, K., Rezvani, Z., and Massoumi, B., *Dyes Pigments*, 2007, vol. 75, no. 3, p. 653.
2. Hernandez-Molina, R. and Mederos, A., in *Comprehensive Coordination Chemistry II*, Lever, A.B.P, Ed., Amsterdam-Oxford-New York: Elsevier-Pergamon, 2003, vol. 2, p. 411.
3. Vigato, P.A., Tamburini, S., and Bertelo, L., *Coord. Chem. Rev.*, 2007, vol. 251, nos. 11–12, p. 1311.
4. Vigato, P.A. and Tamburini, S., *Coord. Chem. Rev.*, 2004, vol. 248, nos. 17–20, p. 1717.
5. Morkovnik, A.S., Divaeva, L.N., Uraev, A.I., et al., *Izv. Akad. Nauk, Ser. Khim.*, 2008, no. 7, p. 1467.
6. Burlov, A.S., Uraev, A.I., Matuev, P.V., et al., *Russ. J. Coord. Chem.*, 2008, vol. 34, no. 12, p. 904.
7. Burlov, A.S., Antsyshkina, A.S., Sadikov, G.G., et al., *Russ. J. Coord. Chem.*, 2000, vol. 26, no. 9, p. 648.
8. USSR Inventor's Certificate no. 682521, *Byull. Izobret.*, 1982, no. 45.
9. USSR Inventor's Certificate no. 979349, *Byull. Izobret.*, 1982, no. 45.
10. Chigarenko, G.G., Ponomarenko, A.G., and Burlov, A.S., *Trenie Iznos.*, 2007, vol. 28, no. 4, p. 397.
11. Garnovskii, A.D., Alekseenko, V.A., Burlov, A.S., and Nedzvetskii, V.S., *Zh. Neorg. Khim.*, 1991, vol. 36, no. 4, p. 886.
12. Garnovskii, A.D., Burlov, A.S., Antsyshkina, A.S., and Divaeva, L.N., *Russ. J. Inorg. Chem.*, 1996, vol. 41, no. 1, p. 85.
13. Kogan, V.A. and Shcherbakov, I.N., *Ros. Khim. Zh.*, 2004, vol. 48, no. 1, p. 69.
14. Garnovskii, A.D. and Vasil'chenko, I.S., *Usp. Khim.*, 2005, vol. 74, no. 3, p. 211.
15. Garnovskii, A.D., Vasilchenko, I.S., Garnovskii, D.A., et al., *J. Coord. Chem.*, 2009, vol. 62, no. 2, p. 151.
16. Naeimi, H., Safari, J., and Heidarnezhad, A., *Dyes Pigments*, 2007, vol. 73, no. 2, p. 251.
17. Ispir, E., *Dyes Pigments*, 2009, vol. 82, no. 1, p. 13.
18. Lippard, S.J. and Berg, J.M., *Principles of Bioinorganic Chemistry*, Mill Valley: Univ. Science Books, 1994.
19. Aiello, I., Ghedini, M., Neve, F., and Pucci, D., *Chem. Mater.*, 1997, vol. 9, no. 10, p. 2107.
20. Rezvani, Z., Ghanea, M.A., Nejati, K., and Baghaei, S.A., *Polyhedron*, 2009, vol. 28, no. 14, p. 2913.
21. Li, L., Hua, X., Huang, Y., et al., *Synth. React. Inorg. Met. Org. Chem.*, 2014, vol. 44, p. 291.
22. Halcrow, M.A., *Comprehensive Coordination Chemistry II*, Que, L. and Tolman, W.B., Eds., NewYork: Elsevier-Pergamon, 2003, vol. 8, p. 395.
23. Gütlich, P., Garcia, Y., and Woike, T., *Coord. Chem. Rev.*, 2001, vols. 219–221, p. 839.
24. Burlov, A.S., Nikolaevskii, S.A., Bogomyakov, A.S., et al., *Rus. J. Coord. Chem.*, 2009, vol. 35, no. 7, p. 486.
25. Garnovskii, A.D., Burlov, A.S., Starikov, A.G., et al., *Rus. J. Coord. Chem.*, 2010, vol. 36, no. 7, p. 483.
26. Wang, P., Ming, H., Zhang, J.Y., et al., *Opt. Commun.*, 2002, vol. 203, p. 159.
27. Burlov, A.S., Mashchenko, S.A., Antsyshkina, A.S., et al., *Rus. J. Coord. Chem.*, 2013, vol. 39, no. 12, p. 707.
28. Burlov, A.S., Mashchenko, S.A., Vlasenko, V.G., et al., *Rus. J. Coord. Chem.*, 2015, vol. 41, no. 6, p. 346.
29. Burlov, A.S., Mashchenko, S.A., Vlasenko, V.G., et al., *J. Mol. Struct.*, 2014, vol. 1061, p. 47.
30. Munire, S., Pervin, D., Muhammet, K., et al., *J. Mol. Struct.*, 2015, vol. 1096, p. 64.
31. Raziyeh, A.A. and Saeid, A., *Molecules*, 2012, vol. 17, p. 6434.
32. Chernyshov, A.A., Veligzhanin, A.A., and Zubavichus, Y.V., *Nucl. Instr. Meth. Phys. Res. A*, 2009, vol. 603, p. 95.
33. Newville, M., *J. Synchrotron Rad.*, 2001, no. 8, p. 96.
34. Zabinsky, S.I., Rehr, J.J., Ankudinov, A., et al., *Phys. Rev. B*, 1995, vol. 52, p. 2995.
35. *CrysAlisPro. Agilent Technologies. Version 1.171.36.32.*
36. Sheldrick, G.M., *Program for the Refinement of Crystal Structure*, Göttingen: Univ. of Göttingen, 1997.
37. Allen, F.H., Kennard, O., Watson, D.G., et al., *J. Chem. Soc., Perkin Trans.*, 1987, no. 12, p. S1.
38. Kogan, V.A., Osipov, O.A., Minkin, V.I., and Sokolov, V.P., *Zh. Neorg. Khim.*, 1965, vol. 10, no. 1, p. 83.
39. Garnovskii, A.D., Ponomarenko, A.G., Burlov, A.S., et al., *Russ. J. Gen. Chem.*, 2010, vol. 80, no. 5, p. 982.
40. Garnovskii, A.D., Burlov, A.S., Lysenko, K.A., et al., *Rus. J. Coord. Chem.*, 2009, vol. 35, no. 2, p. 122.
41. Pattanayak, P., Pratihar, J.L., Patra, D., et al., *Eur. J. Inorg. Chem.*, 2007, p. 4263.

Translated by E. Yablonskaya